

Weak-Field Thermal Hall Conductivity in the Mixed State of d -Wave Superconductors

Adam C. Durst, Ashvin Vishwanath, and Patrick A. Lee

Department of Physics, Massachusetts Institute of Technology, Cambridge, Massachusetts 02139

(Dated: June 6, 2002)

Thermal transport in the mixed state of a d -wave superconductor is considered within the weak-field regime. We express the thermal conductivity, κ_{xx} , and the thermal Hall conductivity, κ_{xy} , in terms of the cross section for quasiparticle scattering from a single vortex. Solving for the cross section (neglecting the Berry phase contribution and the anisotropy of the gap nodes), we obtain $\kappa_{xx}(H, T)$ and $\kappa_{xy}(H, T)$ in surprisingly good agreement with the qualitative features of the experimental results for $\text{YBa}_2\text{Cu}_3\text{O}_{6.99}$. In particular, we show that the simple, yet previously unexpected, weak-field behavior, $\kappa_{xy}(H, T) \sim T\sqrt{H}$, is that of thermally-excited nodal quasiparticles, scattering primarily from impurities, with a small skew component provided by vortex scattering.

PACS numbers: 74.25.Fy, 74.60.Ec, 74.72.-h

Thermal Hall conductivity provides the most direct measure of low temperature quasiparticle transport in a d -wave superconductor. Since quasiparticles are part electron and part hole, their energy is well defined but their charge is not. Thus, it is thermal current that follows quasiparticle current. The longitudinal thermal conductivity, κ_{xx} , has both an electronic and a phononic contribution. However, the thermal Hall conductivity, κ_{xy} , induced by a perpendicular magnetic field (the Righi-Leduc effect), is purely electronic in origin and the direct consequence of a transverse quasiparticle current.

Over the past few years, much progress has been made in measuring the thermal Hall conductivity of the cuprate superconductors in the mixed (vortex) state, $H_{c1} < H < H_{c2}$ [1, 2, 3, 4]. Most recently, Ong and co-workers [4] measured κ_{xy} in high-purity single crystals of slightly overdoped ($T_c = 89$ K) $\text{YBa}_2\text{Cu}_3\text{O}_{6.99}$ (YBCO). Their data indicates that, for magnetic fields up to 14 Tesla and temperatures between 15 K and 28 K, κ_{xy}/T^2 is only a function of the ratio \sqrt{H}/T . This is in agreement with the scaling theory proposed by Simon and Lee [5] which predicts that, for nodal quasiparticles with a Dirac-like dispersion, $\kappa_{xy}(H, T) \sim T^2 F_{xy}(\sqrt{H}/\gamma T)$ where $\gamma = (k_B/v_f)\sqrt{c/\hbar e}$ and $F_{xy}(x)$ is a general scaling function. Furthermore, the experiments show that for $\sqrt{H} \ll \gamma T$ the measured scaling function has the surprisingly simple form, $F_{xy}(x) \sim x$, such that $\kappa_{xy}(H, T) = C_0 T \sqrt{H}$ where C_0 is a constant. For larger magnetic fields, the measured curves peak and then decrease. It is unusual to see \sqrt{H} (rather than H) in a Hall response and this interesting result was theoretically unexpected. Yet such a simple functional form must have a simple explanation. In this Letter, we seek to provide it.

The key to this problem is that we are dealing with the *high* temperature regime of low T quasiparticle transport. By low T quasiparticle transport, we mean that quasiparticles are excited only in the vicinity of gap nodes and inelastic scattering can be neglected. (Quasiparticle dispersion is therefore given by the anisotropic Dirac spectrum, $E = (v_f^2 k_1^2 + v_2^2 k_2^2)^{1/2}$, where v_f is the Fermi

velocity, v_2 is the slope of the gap, and k_1 and k_2 are defined locally about each node. With our choice of axes, gap nodes are located at $\pm p_F \hat{x}$ and $\pm p_F \hat{y}$ in momentum space.) However, the experiments involve temperatures large compared to the impurity scattering rate and the vortex scattering rate. As a result, the quasiparticles responsible for transport are thermally generated rather than impurity-induced [6, 7, 8] or magnetic field-induced [9, 10]. (Note that thermal transport in the opposite, low T , regime has been discussed frequently in the recent literature [11, 12, 13, 14, 15].) This high T regime is relatively simple. To understand the thermal conductivity, we need only understand how the thermally excited quasiparticles scatter from impurities and magnetic vortices.

In the presence of a magnetic field ($H_{c1} < H \ll H_{c2}$), vortices penetrate the sample (a 2D CuO_2 layer). They are distributed randomly, pinned to local defects. The cuprates are extreme type II superconductors in which the coherence length, ξ , is much smaller than the penetration depth, λ . As a result, while the vortex cores may be well separated, the magnetic field profiles overlap significantly such that there is little variation in the magnetic field across the sample. We therefore adopt the extreme type II limit of $\xi \rightarrow 0$ and $\lambda \rightarrow \infty$ and take the magnetic field to be constant, $\mathbf{H} = H\hat{z}$. In this limit, there are only two remaining length scales. The first, $1/k$, is set by the temperature such that $k \equiv E/\hbar v_f = k_B T/\hbar v_f$. The second length scale, R , is half of the average distance between vortices. With one flux quantum per vortex, $H\pi R^2 = \Phi_0 = hc/2e$, so we define $R \equiv \sqrt{\hbar c/eH}$. In terms of R , we can define the (2D) density of vortices to be $n_v = H/\Phi_0 = 1/\pi R^2$. The ratio of the two length scales yields $kR = \gamma T/\sqrt{H}$, which is the inverse of the argument of the scaling functions.

We consider nodal quasiparticles carrying a heat current in response to a thermal gradient in the x -direction. Defining a mean free path, ℓ , we can express κ_{xx} in terms of the electronic specific heat, C_v , via $\kappa_{xx} = v\ell C_v/2$ where v is the average quasiparticle velocity [16]. Specific

heat in the mixed state has been calculated by Kopnin and Volovik [10]. For magnetic fields small compared to the temperature, they find $C_v \sim T^2[1 + \mathcal{O}((\sqrt{H}/\gamma T)^2)]$. The second term, a measure of the magnetic field contribution to quasiparticle generation, can be neglected in the regime of interest. Doing so and defining a thermal Hall angle, $\tan\theta_H \equiv \kappa_{xy}/\kappa_{xx}$, yields a simple form for the thermal conductivity: $\kappa_{xx}/T = \alpha_0 k\ell$ and $\kappa_{xy}/T = \alpha_0 k\ell \tan\theta_H$, where $\alpha_0 \approx 1.72 k_B^2 v/\hbar v_2$ times the stacking density of CuO₂ planes.

The mean free path has contributions from both impurity scattering and vortex scattering. For small impurity densities and dilute vortices, we expect these to be relatively independent. Thus, via Matthiessen's rule, we write $1/\ell = 1/\ell_0 + 1/\ell_v$ where ℓ_0 and ℓ_v are the contributions from impurities and vortices respectively. Since $1/\ell_v$ vanishes for $H = 0$, ℓ_0 can be found empirically from $\kappa_e(T)$, the electronic part of $\kappa_{xx}(H = 0)$. We define $A \equiv k\ell_0 = \kappa_e(T)/\alpha_0 T$. As argued by Simon and Lee [5], we expect scaling even in the presence of disorder as long as the impurity scattering does not yield an additional length scale (as for δ -correlated disorder). If so, then A must be T -independent. (Note that it is a different constant from that obtained in the universal limit [8].) Zero-field measurements of κ_{xx} in YBCO [2, 17] show that this is realized experimentally for $T < 30$ K, which is precisely the temperature range over which the κ_{xy} data obeys scaling.

Now consider the vortex contribution. Superflow circulates about the vortices, falling off like $1/r$ near the center of each vortex and cancelling with superflow of opposite direction (circulating about neighboring vortices) in the regions between vortices. We therefore attribute to each vortex the circulating superflow in the area that surrounds it. Since the vortex scattering should depend primarily on the average vortex density and be relatively insensitive to higher order details of the vortex configuration, we can approximate the exact superflow distribution by cutting off the superflow about each vortex at a distance R from its center. In this manner, we define an effective single vortex for which we have approximately accounted for the influence of neighboring vortices. If we assume that scattering events from such vortices are otherwise uncorrelated, then we can express ℓ_v in terms of the single vortex transport cross section, $\sigma_{||}$, and the density of vortices, n_v . In this approximation, the transport scattering rate is $1/\tau_v = n_v v \sigma_{||}$ and, since $\ell_v = v \tau_v$, we find $\ell_v = 1/n_v \sigma_{||} = \pi R^2/\sigma_{||}$. Since vortices are endowed with a circulation, the vortex scattering cross section can have a small skew component, σ_{\perp} . Thus, when a quasiparticle encounters a vortex, it has a slightly greater probability of scattering to one side than the other and thereby contributes to J_y . This process repeats with each successive vortex until the quasiparticle has travelled a distance equal to its mean free path. Therefore, given a heat current, J_x , we can express the transverse heat

current as $J_y = J_x n_v \sigma_{\perp} \ell$. The thermal Hall angle is then given by $\tan\theta_H = \kappa_{xy}/\kappa_{xx} = -J_y/J_x = -\sigma_{\perp} \ell/\pi R^2$ where we used $\kappa_{xy} = -\kappa_{yx}$.

Combining our results to this point, we find that κ_{xx} and κ_{xy} can be expressed in terms of the single vortex scattering cross section via

$$\frac{\kappa_{xx}}{\alpha_0 T} \equiv F_{xx}(x) = \frac{1}{\frac{1}{A} + \frac{1}{\pi} x^2 f_{||}\left(\frac{1}{x}\right)} \quad (1)$$

$$\frac{\kappa_{xy}}{\frac{\alpha_0 k_B}{2E_F} T^2} \equiv F_{xy}(x) = \frac{\frac{1}{\pi} x^2 f_{\perp}\left(\frac{1}{x}\right)}{\left(\frac{1}{A} + \frac{1}{\pi} x^2 f_{||}\left(\frac{1}{x}\right)\right)^2} \quad (2)$$

where $x \equiv 1/kR = \sqrt{H}/\gamma T$, $E_F \equiv v_f p_F/2$, and we have defined dimensionless functions of $kR = 1/x$ such that $k\sigma_{||} \equiv f_{||}(kR)$ and $k\sigma_{\perp} \equiv -(k/p_F) f_{\perp}(kR)$. The extra factor of k/p_F in the definition of f_{\perp} reflects the fact that κ_{xy} is small by a factor of $k_B T/E_F$ [5].

Next, we calculate $f_{||}(kR)$ and $f_{\perp}(kR)$ by considering the quantum mechanical scattering of a quasiparticle from a single vortex. Our calculation, the details of which will be presented elsewhere [18], is similar in spirit to that conducted by Cleary [19] for the case of an s -wave superconductor. We consider the Bogoliubov-de Gennes (BdG) equation for a d -wave superconductor in the presence of a single vortex. We apply a singular gauge transformation that simplifies the BdG Hamiltonian at the cost of imposing antiperiodic boundary conditions which require that our wave function change sign with each trip around the vortex. We further simplify by shifting the origin of momentum space to the location of one of the gap nodes and neglecting scattering from one node to another. (This is physically reasonable since the superflow from which quasiparticles scatter is smooth on the scale of $1/p_F$.) The resulting problem is one of an (anisotropic) Dirac fermion scattering from an effective non-central potential (due to the superflow) in the presence of antiperiodic boundary conditions and small, yet important, curvature terms in the Hamiltonian.

Quasiparticles interact with vortices via the superflow as well as the Berry phase factor of (-1) acquired upon circling a vortex. This phase is encoded in the antiperiodic boundary conditions imposed on quasiparticles in our chosen gauge. We make the following approximations. First, we neglect the Berry phase effect and instead adopt periodic boundary conditions for the quasiparticle, which is equivalent to considering the case of an $\hbar c/e$ (double) vortex. To justify this, we note that the Berry phase only affects quasiparticle trajectories that lie within the thermal deBroglie wavelength of the vortex core, such that two paths that pass on either side of the core can interfere. Thus, any additional contribution to the cross section can at best equal the deBroglie wavelength. Since this wavelength is much smaller than the spacing between vortices (for $\sqrt{H} \ll \gamma T$), the Berry

phase contribution may change the size of the cross section, but should not change its dependence on magnetic field. Second, we assume an isotropic Dirac dispersion in the linearized Hamiltonian, which allows us to more easily work with angular momentum eigenstates and simplifies the calculation. This is clearly an approximation for the cuprates where v_f exceeds v_2 by a factor of 10 to 20 [20]. Third, we approximate the effect of neighboring vortices by cutting off the superflow distribution about our single vortex at a distance R from its center. By construction, the flux through this circle is exactly one $(hc/2e)$ flux quantum. The resulting superfluid momentum (superflow) is $\mathbf{P}_s(\mathbf{r}) = (\hbar/2)(1/r - r/R^2)\theta(R-r)\hat{\phi}$. The BdG Hamiltonian (for quasiparticles about the node at $+p_F\hat{x}$) is then given by the sum of a linearized (Dirac) part, $H_D = v_f[\tau_3 p_x + \tau_1 p_y + P_{sx}]$, and a quadratic (curvature) part, $H_C = (v_f/2p_F)[\tau_3(p^2 + P_s^2) + 2\mathbf{P}_s \cdot \mathbf{p} + \tau_1(2p_x p_y)]$, which is small sufficiently far from the vortex center ($r > 1/p_F$). Since we cutoff our model at the scale of the vortex core ($\xi \sim 10/p_F$), curvature terms can be considered perturbatively. Finally, we select a reasonable core size and model the vortex core as a region with vanishing superflow; which is the best we can do in the absence of further experimental input. We now have a well-defined scattering problem, which is first solved considering the linearized Hamiltonian, and then perturbed to first order in the curvature terms. (Note, if curvature terms are neglected completely, there is no skew scattering [5, 13, 14].) Due to these approximations, we cannot expect our results to be quantitative. Yet, the qualitative agreement with experiment is surprisingly good, which indicates that we have retained the essential physics.

Note that H_D includes an effective non-central potential, $V = -v_f P_s(r) \sin \phi$. This mixes angular momentum eigenstates and requires that we solve for all of them simultaneously. We do so numerically, including the contributions of up to 46 angular momenta. Given the eigenstates both inside ($r < R$) and outside ($r > R$) the vortex, we apply boundary conditions at the origin, match solutions at the vortex edge ($r = R$), and construct a wave function composed of an incident plane wave and an outgoing radial wave. The angular prefactor of the radial piece yields the differential cross section. Summing over contributions from each of the four nodes and integrating over scattering angles, we obtain the total cross section, $\sigma = \int d\varphi (d\sigma/d\varphi)$, the transport cross section, $\sigma_{\parallel} = \int d\varphi (1 - \cos \varphi) (d\sigma/d\varphi)$, and the skew cross section, $\sigma_{\perp} = \int d\varphi \sin \varphi (d\sigma/d\varphi)$.

Results for a range of intervortex distances, $kR = \gamma T/\sqrt{H}$, from 0.5 to 15, are plotted in Fig. 1. Note that while σ and σ_{\parallel} are plotted in units of $1/k$, σ_{\perp} is plotted in units of $-1/p_F$. This reflects the fact that the skew cross section, induced by the curvature terms of the Hamiltonian, is small by a factor of k/p_F . The minus sign indicates that the quasiparticles get deflected to the right, just as an electron would in response to the

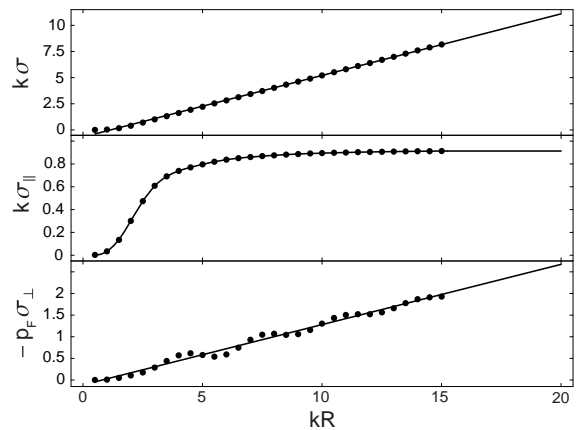


FIG. 1: Calculated total, transport, and skew cross sections as a function of kR from 0.5 to 15. For σ and σ_{\perp} , solid lines are fits to straight lines with small negative intercepts. For σ_{\parallel} , the solid line is an interpolation of the numerical data in which the constant large- kR behavior is extrapolated to larger kR . The oscillating component of the σ_{\perp} data is believed to be a numerical artifact.

Lorentz force. For large kR , $k\sigma$ and $-p_F\sigma_{\perp}$ increase linearly with kR while $k\sigma_{\parallel}$ saturates to a constant value.

The form of σ and σ_{\parallel} can be understood in terms of a simple Born-limit calculation [18]. The 2D Fourier transform of $1/r$ yields (approx) $1/q$ and squares to yield $d\sigma/d\varphi \sim k/q^2$ where $q^2 = |\mathbf{k} - \mathbf{k}'|^2 = 2k^2(1 - \cos \varphi)$. Since $1/(1 - \cos \varphi)$ diverges for small angles, angular integration is dominated by the small angle cutoff at $q \approx 1/R$ and yields $\sigma \sim R$. By contrast, since the extra factor of $(1 - \cos \varphi)$ in the definition of σ_{\parallel} precisely cancels this divergence, we obtain $\sigma_{\parallel} \sim 1/k$. A nonzero σ_{\perp} , however, can only be obtained by going beyond the Born limit.

We can now use the fits to these numerical results as the input to Eqs. (1) and (2). The other input, $A \equiv \kappa_e(T)/\alpha_0 T$, is obtained empirically from the measured zero-field thermal conductivity in YBCO (extrapolated for the lowest T) [17]. This quantity is a T -independent constant for $T < 30$ K but decreases for larger T where inelastic scattering becomes significant. Our calculated thermal conductivities are plotted (in scaling form) in Fig. 2. In each plot we show 15 curves for T ranging from 15 K to 70 K. The low T curves (for which $A \approx \text{const}$) satisfy scaling and therefore lie nearly on top of each other. At higher T , the curves deviate from scaling, presumably due to the onset of inelastic scattering. Both the functional form of the scaling curves and the manner in which scaling is violated agree qualitatively with the mixed state thermal conductivity data measured in YBCO by Ong and co-workers [4].

The form of our scaling curves can be understood as follows. In the small H regime, the mean free path is dominated by impurity scattering ($\ell_0 \ll \ell_v$). Since $x = 1/kR = \sqrt{H}/\gamma T$ is small, the cross sections take on their

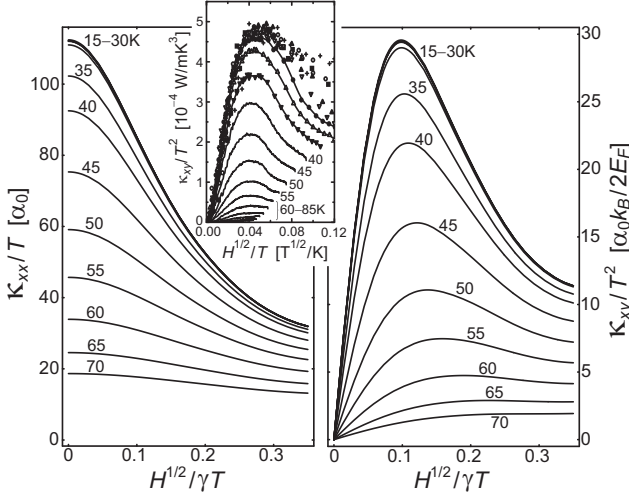


FIG. 2: Calculated longitudinal thermal conductivity (left) and thermal Hall conductivity (right) plotted in scaling form (in units defined in the text). The inset is the measured thermal Hall conductivity (in SI units) obtained by Ong and co-workers for $\text{YBa}_2\text{Cu}_3\text{O}_{6.99}$ and reproduced here from Ref. 4.

simple large- kR form, $f_{\parallel}(1/x) \approx c_{\parallel}$ and $f_{\perp}(1/x) \approx c_{\perp}/x$, where c_{\parallel} and c_{\perp} are constants. Therefore, the scaling functions are $F_{xx}(x) = A$ and $F_{xy}(x) = c_{\perp}A^2x/\pi$ and we find that the weak-field thermal Hall conductivity is

$$\kappa_{xy}(H, T) = C_0 T \sqrt{H} \quad (3)$$

where $C_0 \equiv \alpha_0 k_B c_{\perp} A^2 / 2\pi \gamma E_F$. (For reasonable parameter values, this yields $C_0 = 7.2 \times 10^{-3} \text{W/mK}^2 \sqrt{\text{Tesla}}$ which is only a factor of 2 smaller than the experimental value reported in Ref. 4.) As H grows, vortex scattering increases, increasing the skew scattering while reducing ℓ (and therefore κ_{xx}). Near the point where $\ell_0 \approx \ell_v$, the competition between the decreasing mean free path and the increasing skew scattering results in a peak for the κ_{xy} scaling curve. If the impurity scattering is sufficiently weak, this peak can occur for small enough H that the cross sections still take their simple large- kR forms. Thus, for sufficiently clean samples, at temperatures where scaling is satisfied, it follows from Eq. (2) that the peak height and location should be proportional to $A^{3/2}$ and $A^{-1/2}$ respectively. Recall, as well, that $C_0 \sim A^2$. These are predictions that can be checked experimentally by comparing results for samples of differing purity. Once vortex scattering dominates the mean free path ($\ell_0 \gg \ell_v$), κ_{xy} decreases with increasing H . As we push this model toward the strong-field (large x) regime, the transport cross section decreases from its large- kR value, increasing ℓ and causing a leveling out and eventual upturn in the scaling curves for both κ_{xx} and κ_{xy} . However, in this strong-field regime ($\sqrt{H} \gtrsim \gamma T$), there is a magnetic field contribution to the quasiparticle density of states and so our picture of thermally-excited quasiparticles scattering from dilute vortices ceases to be valid.

Note in particular, that the simple, yet previously unexpected, form of the weak-field thermal Hall conductivity, $\kappa_{xy} \sim T\sqrt{H}$, is now easily understood. Summarizing the preceding discussion, we write $\kappa_{xx} \sim C_v \ell$ and $\kappa_{xy} \sim \kappa_{xx} n_v \sigma_{\perp} \ell \sim C_v \ell^2 n_v \sigma_{\perp}$. In the weak-field limit, since quasiparticles are thermally excited, $C_v \sim T^2$. For small magnetic fields, the mean free path is dominated by impurity scattering. Therefore $\ell \sim \ell_0 \sim \kappa_e(T)/C_v \sim 1/T$. The vortex density is just proportional to the magnetic field, $n_v \sim H$. Our numerics yield $\sigma_{\perp} \sim (k/p_F)R \sim T/\sqrt{H}$, which says that, aside from being small by a factor of k/p_F , the skew cross section is just proportional to the effective vortex radius, R . Putting it all together yields $\kappa_{xy} \sim (T^2)(1/T)^2(H)(T/\sqrt{H}) \sim T\sqrt{H}$. The simple form of this result is due to the simple nature of the weak-field regime. Here we have thermally excited quasiparticles with a mean free path due to impurity scattering. The only effect of the vortices is to add a small skew component to the scattering. The unusual \sqrt{H} Hall response results because, while the number of vortices goes like H , the skew cross section per vortex goes like $1/\sqrt{H}$.

While our analysis appears to yield the correct functional form of the thermal conductivity, we do not expect our results to be quantitative due to the approximations we made in calculating the single vortex cross section. To obtain more quantitative results, one must include the Berry phase contribution, consider anisotropic Dirac nodes, and account (via empirical input) for the details of the vortex core. This is left for future work.

We are very grateful to Y. Zhang and N. P. Ong for sending us their unpublished κ_{xx} data and allowing us to reproduce their κ_{xy} plot in Fig. 2. We thank D. Huse, A. Millis, T. Senthil, and J. Ye for helpful discussions. This work was supported by NSF Grant No. DMR-0201069. A. V. was supported by an MIT Pappalardo Fellowship.

-
- [1] K. Krishana *et al.*, Phys. Rev. Lett. **82**, 5108 (1999)
 - [2] N. P. Ong *et al.*, cond-mat/9904160 (unpublished)
 - [3] R. Ocana *et al.*, J. Low Temp. Phys. **123**, 181 (2001)
 - [4] Y. Zhang *et al.*, Phys. Rev. Lett. **86**, 890 (2001)
 - [5] S. H. Simon and P. A. Lee, Phys. Rev. Lett. **78**, 1548 (1997)
 - [6] P. A. Lee, Phys. Rev. Lett. **71**, 1887 (1993)
 - [7] M. J. Graf *et al.*, Phys. Rev. B **53**, 15147 (1996)
 - [8] A. C. Durst and P. A. Lee, Phys. Rev. B **62**, 1270 (2000)
 - [9] G. E. Volovik, Pis'ma Zh. Eksp. Teor. Fiz. **58**, 457 (1993) [JETP Lett. **58**, 469 (1993)]
 - [10] N. B. Kopnin and G. E. Volovik, Pis'ma Zh. Eksp. Teor. Fiz. **64**, 641 (1996) [JETP Lett. **64**, 690 (1996)]
 - [11] M. Franz, Phys. Rev. Lett. **82**, 1760 (1999)
 - [12] I. Vekhter and A. Houghton, Phys. Rev. Lett. **83**, 4626 (1999)
 - [13] J. Ye, Phys. Rev. Lett. **86**, 316 (2001)
 - [14] A. Vishwanath, Phys. Rev. Lett. **87**, 217004 (2001); Phys. Rev. B **66**, 64504 (2002)

- [15] O. Vafek *et al.*, Phys. Rev. B **64**, 224508 (2001)
- [16] Note that for an energy-dependent ℓ , this simple relation between κ_{xx} and C_v is only approximate. We verified that while the more exact relation (see Ref. 18) modifies details, it preserves the qualitative form of our results.
- [17] Y. Zhang and N. P. Ong (private communication)
- [18] A. C. Durst *et al.* (in preparation)
- [19] R. Cleary, Phys. Rev. **175**, 587 (1968)
- [20] M. Chiao *et al.*, Phys. Rev. B **62**, 3554 (2000)